Available online at www.sciencedirect.com
SCIENCE DIRECT®
Thermochimica Acta 402 (2003) 199–208
thermochimica acta
www.elsevier.com/locate/tca

Kinetics of the thermal decomposition of CuC_2O_4–ZnC_2O_4 mixture in air

M.A. Gabal

Chemistry Department, Faculty of Science, Benha University, Benha, Egypt

Received 15 August 2002; received in revised form 3 December 2002; accepted 4 December 2002

Abstract

The thermal decomposition processes taking place in the solid state oxalate mixture of CuC_2O_4–$ZnC_2O_4{\cdot}2H_2O$ (1:1 mole ratios) have been studied in air using DTA–TG, XRD and SEM techniques. DTA–TG curves showed that, the decomposition proceeds through three well-defined steps with DTA peaks closely correspond to the weight loss obtained. The decomposition behaviour of the oxalate mixture is in good agreement with that of the individual oxalates. XRD showed an increase in the intensity of the diffraction lines on rising the calcinations temperature from 400 to 800 °C attributed to the grain growth of the decomposition products. SEM experiments confirmed this result as the very small crystallites obtained at 400 °C are re-textured and coalesced into aggregates of large crystals with sharp edges and angles when calcined at 800 °C. Kinetic analysis of the oxalate decomposition steps was performed under non-isothermal conditions using different integral methods of analysis. The dynamic TG curves obeyed the Avrami–Erofeev equation characteristic of solid-state nucleation-growth mechanism and consistent with the textural changes accompanying the decomposition revealed by SEM experiments. The activation parameters were calculated and discussed in view of the electronegativity of the metal ions.

Keywords: Copper oxalate; Zinc oxalate; DTA–TG; SEM; Kinetic

1. Introduction

Investigation of chemical, physical and structural properties of mixed metal oxides have found very important applications in new technologies. They can be used as prospective materials for superior technical ceramics, materials for magnetic recording, many electronic components, sensors, catalysts as well as the high-temperature superconductors.

CuO/ZnO catalyst was used for the catalytic generation of hydrogen from the reaction of methanol with oxygen in the presence of steam [1]. Heterocontact gas sensor with layered structure of CuO/ZnO was introduced to enhance the sensitivity and selectivity to CO gas [2]. CuO supported on ZnO prepared by the impregnation of basic zinc carbonate with a water solution of copper nitrate followed by heat treatment at different temperatures was found to possess surface and catalytic properties depend upon CuO content and the calcination temperature [3].

The thermal decomposition of copper oxalate differs substantially from that of the other transition metal oxalates since it exhibits a strongly exothermic reaction with the formation of copper metal when heated in nitrogen and this reaction is described as autocatalytic. In oxygen, the overall reaction is strongly exothermic,

E-mail address: mgabalabdo@yahoo.com (M.A. Gabal).

0040-6031/03/$ – see front matter © 2003 Elsevier Science B.V. All rights reserved.
doi:10.1016/S0040-6031(02)00616-0

owing to oxidation of the evolved CO to CO_2 beside the oxidation of metal to metal oxide [4].

Dollimore and coworkers [4,5] studied the thermal decomposition of $ZnC_2O_4{\cdot}2H_2O$ in air and nitrogen and found that the end product in both atmospheres is ZnO.

Many researchers have paid their attention to the different synthesis methods of the mixed metal oxides and their characterization. Mixed cerium–gadolinium oxalates [6] have been used as precursors for the preparation of important materials exhibiting high ionic conductivity. The thermal behaviour of the coprecipitated mixed metal oxalates [7]; $MCu(C_2O_4)_2{\cdot}xH_2O$ where M: Fe, Co or Ni examined in air and nitrogen atmospheres showed that, their thermal behavior is differed from that of the individual metal oxalates.

Thermal techniques have been used for studying the kinetics of the thermal decomposition reactions of solids. In analyzing the kinetic data it is true that, the conventional isothermal method is important for estimating the kinetic model but the dynamic method has some advantages over it in several respects [8].

The kinetics of copper oxalate [9] decomposition reaction showed that the decomposition obeyed the Avrami–Erofeev (A_2) mechanism when studied by isothermal and rising temperature experiments in both nitrogen and air atmospheres.

Yankwich and Zavitsanos [10] have been reported the activation energies for zinc oxalate decomposition reaction, based on the observed pressure of the gaseous products during the decomposition, assuming different reaction interface models.

In the present study, the thermal decomposition of physical oxalate mixture of CuC_2O_4–$ZnC_2O_4{\cdot}2H_2O$ (1:1 mole ratios) in air has been studied using DTA–TG techniques. The parent mixtures and mixtures calcined at different temperatures were characterized using XRD and SEM techniques to gave some information about the decomposition products. Kinetic analysis of TG data were performed and considered with reference to the various models and computational methods of solid state reactions. The results of various techniques used to examine the chemical phases, morphology and texture changes that occur during the thermal decomposition and the kinetics of the decomposition reactions are compared and discussed.

2. Experimental

2.1. Materials

Individual metal oxalates were prepared by precipitation from aqueous solutions containing the calculated amounts of AR metal chloride salt with equimolar quantity of AR oxalic acid. The fine precipitate obtained were filtered, washed with distilled water until free of chloride ions and dried.

Physical mixture of CuC_2O_4–$ZnC_2O_4{\cdot}2H_2O$ (1:1 mole ratios) was prepared using the impregnation technique [11]. Bidistilled water was added in drops to the appropriate mole ratios of the two metal oxalates with vigorous stirring to assure complete homogeneity. The wetted oxalates mixture was then dried in a thermostatic oven at 100 °C for about 2 h.

2.2. Experimental apparatus

Simultaneous DTA–TG experiments were performed using a Shimadzu DT-40 thermal analyzer. Experiments were carried out in air at flow rate of $30\,l\,h^{-1}$ against α-alumina as a reference, at heating rates of 1, 2, 3 and $5\,^{\circ}C\,min^{-1}$. The sample mass in the Pt cell of the thermal analyzer was kept at about 8 mg in all experiments, in order to ensure a linear heating rate and accurate temperature measurements.

In accordance with DTA–TG results, samples of the oxalates mixture were thermally heated in an electrical oven at different temperatures for specified durations then removed and cooled in a desiccators to room temperature.

XRD patterns for the different calcined samples were recorded at room temperature using a Philips PW 1710 X-ray diffraction unit using a Cu target and Ni filter.

The changes in morphology and texture taking place during the thermal decomposition of the mixture were investigated using a Jeol T 300 scanning electron microscope.

3. Results and discussion

3.1. DTA–TG

Fig. 1 shows the DTA–TG curves in air at heating rate of $5\,^{\circ}C\,min^{-1}$ for CuC_2O_4–$ZnC_2O_4{\cdot}2H_2O$

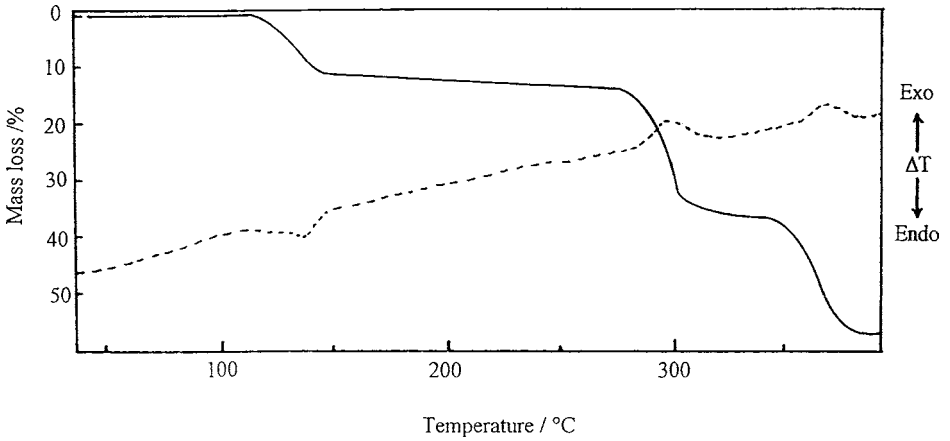

Fig. 1. DTA–TG curves of CuC_2O_4–$ZnC_2O_4{\cdot}2H_2O$ (1:1 mole ratios) mixture in air at heating rate of 5 °C min^{-1}.

mixture (1:1 mole ratios). The DTA peaks closely correspond to the weight changes observed on the TG curves. The DTA–TG curves show that, the thermal decomposition of the mixture at temperatures below 400 °C occurs in three well-defined steps. The first step starts at about 112 °C, characterized by a broad endothermic DTA peak at 132 °C and is accompanied by a weight loss of 11% at 170 °C in accordance with calculated weight loss of 10.6% attributed for the dehydration of $ZnC_2O_4{\cdot}2H_2O$ and the formation of anhydrous oxalate mixture. The mixture is stable up to about 260 °C, and is then decomposed in the second step. This step shows an exothermic process with broad DTA peak at 300 °C, indicating a weight loss of 22% in accordance with calculated weight loss 21.1% due to the decomposition of CuC_2O_4 and the formation of CuO–ZnC_2O_4 mixture. The third decomposition step is also exothermic with DTA peak at about 360 °C, accompanied by a weight loss of 21.5% compared with theoretical weight loss of 21.1% attributed to the decomposition of ZnC_2O_4 in the mixture and the formation of CuO–ZnO mixture at 390 °C.

From the above results it is clear that the DTA–TG behavior of the metal oxalates in their physical mixture are in general agreement with those reported for the individual metal oxalates [4,5,7]. In other words, the thermal decomposition behaviors of the metal oxalates are not much affected by their presence in the mixture and each one behaves as it is present alone. A similar behavior was found by Coetzee et al. [7] where TG and DSC results on ground physical mixtures of copper oxalate with iron(II) oxalate, cobalt oxalate or nickel oxalate indicate that the dehydration, the decomposition in nitrogen and the reactions in oxygen are the same as those of the individual oxalates. The obtained dehydration temperature of $ZnC_2O_4{\cdot}2H_2O$ suggests that the water molecules are present as crystalline water [12]. The exothermic character of the DTA peaks accompanying the oxalate decomposition steps is due to the air oxidation of CO to CO_2. The enthalpy change associated with this reaction has to be higher than the endothermic heat required to drive off CO [5].

The obtained data also indicates the temperatures equivalent to the theoretical weight loss which can be selected as the minimum temperatures for the calcination processes. Thus, samples of CuC_2O_4–$ZnC_2O_4{\cdot}2H_2O$ mixture were calcined at 320 °C for 30 min, at 400 °C for 1 h or at 800 °C for 2 h.

XRD and SEM experiments were carried out for the parent mixture and mixtures calcined at different temperatures to characterize the decomposition products at different stages.

3.2. X-ray diffraction

The starting mixture gave XRD pattern in general agreement with the results reported in the ASTM data cards for CuC_2O_4 and $ZnC_2O_4{\cdot}2H_2O$. In accordance with DTA–TG results, the mixture calcined at 320 °C shows the XRD lines characteristic of CuO and the disappearance of any XRD lines characteristic

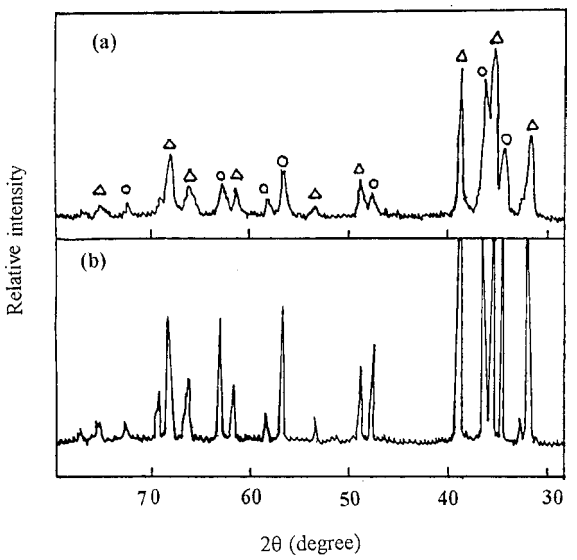

Fig. 2. Characteristic parts of XRD patterns of CuC_2O_4–ZnC_2O_4·$2H_2O$ (1:1 mole ratios) mixture calcined at 400 °C (a) and 800 °C (b). Phases: (△) CuO and (○) ZnO.

of CuC_2O_4. Fig. 2 shows the characteristic parts of the X-ray powder diffraction patterns for the mixture calcined at 400 and 800 °C. The XRD pattern of the mixture calcined at 400 °C (Fig. 2a) gave the characteristic lines of metal oxide mixture, CuO–ZnO. The small broadening of the diffraction lines obtained indicate the poorly crystalline structure at this decomposition stage. For the mixture calcined at 800 °C (Fig. 2b), the increase in the intensities of XRD lines, without changing their position, which was accompanied by a change in the color of the mixtures compared with those obtained at 400 °C can be attributed to the grain growth and the formation of well-crystallized oxide mixture. A similar behavior was found by Osvaldo et al. [13] for $(ZnO)_x(CdO)_{1-x}$ thin films prepared with different compositions by spray pyrolysis on glass substrates and exposed to different annealing treatment, where the crystallite sizes were found to increase with annealing.

3.3. Scanning electron microscope

SEM of the parent mixture are not produced here because the crystallite of the reactants were too small (<0.5 μm) to permit satisfactory resolution of textural features. Picture quality was often poor due to charge retention arising from the low electrical conductivity of the porous aggregates that constituted the particle assemblages. Mohamed and Galwey [14] showed a similar behavior for copper(II) oxalate on the studying kinetic and mechanistic studies of its thermal decomposition.

The SEM micrographs showing the changes in morphology and texture that accompany the thermal decomposition of CuC_2O_4–ZnC_2O_4·$2H_2O$ mixture in air are shown in Fig. 3. The results show that the particle shape and size change throughout the decomposition process. Micrograph of the mixture calcined at 320 °C (Fig. 3a) shows two types of crystals. The first type was attributed to the decomposition of copper oxalate and breaking into small and fine granules with roughening of the crystal surfaces. The other type showing relatively large crystals of different size and shape, assigned to cadmium oxalate. Micrograph of the mixture calcined at 400 °C (Fig. 3b) shows the complete breaking into very small and fine granules of the crystal surface due to the decomposition of cadmium oxalate crystals in the mixture. Micrograph of the mixture calcined at 800 °C (Fig. 3c) shows a re-texturing and coalescence into aggregates of hexagonal large crystals of different sizes with sharp edges and angles. The results of SEM experiments are thus consistent with the results of XRD analysis.

3.4. Kinetic studies

The kinetics of the oxalate decomposition steps (viz. the last two decomposition steps) have been studied under dynamic conditions using heating rates of 1, 2, 3 and 5 °C min^{-1}. Kinetic analysis of the dynamic TG curves were carried out using three integral methods: the Ozawa method [15], the Coats–Redfern method [16] and Diefallah's composite method [12] which is based either on the modified Coats–Redfern equation [16]; (composite method I) or on the Doyle's equation [17]; (composite method II).

With dynamic techniques, the temperature rate is set to a constant value β and the function $g(\alpha)$ is given by Doyle's equation [17]:

$$g(\alpha) = \frac{A}{\beta}\int_0^{\infty} \exp\left(-\frac{E}{RT}\right) \mathrm{d}T = \frac{AE}{\beta R} P(\chi) \qquad (1)$$

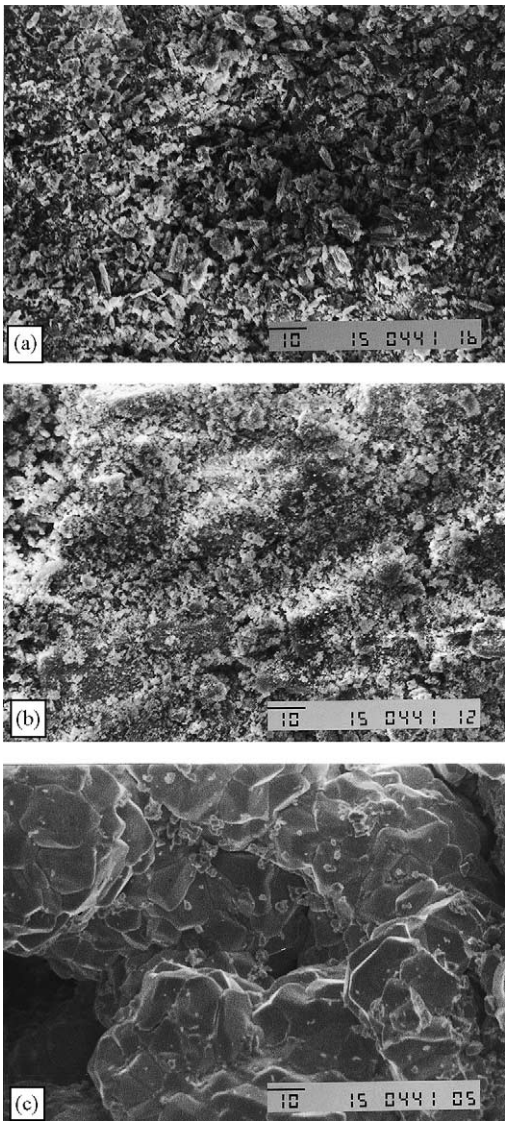

Fig. 3. Scanning electron micrograph showing the changes in texture and morphology that accompany the thermal decomposition of CuC_2O_4–$ZnC_2O_4{\cdot}2H_2O$ (1:1 mole ratios) mixture in air. Mixture calcined at: (a) 320 °C; (b) 400 °C and (c) 800 °C (scale bar 10 μm).

The function $P(\chi)$ has been defined as follows:

$$P(\chi) = \frac{e^{-\chi}}{\chi} - \int_0^{\infty} \frac{e^{-u}}{u}\,du \tag{2}$$

where $u = E/RT$ and χ is the corresponding value of u at which a fraction α of material has decomposed.

In the Coats–Redfern method [16], the function $g(\alpha)$ is approximated to the form:

$$g(\alpha) = \frac{ART^2}{\beta E}\left[1 - \frac{2RT}{E}\right] e^{-E/RT} \tag{3}$$

This equation has been written in the form:

$$-\ln\left[\frac{g(\alpha)}{T^2}\right] = -\ln\frac{AR}{\beta E}\left[1 - \frac{2RT}{E}\right] + \frac{E}{RT} \tag{4}$$

The quantity $\ln(AR/\beta E)(1-(2RT)/E)$ is reasonably constant for most values of E and in the temperature range over which most reactions occur.

In the Ozawa method [15], a master curve has been derived from the TG data obtained at different heating rates (β) using Doyle's equation [17] and assuming that $[(AE/R\beta)P(E/RT)]$ is a constant for a given fraction of material decomposed. The function $P(E/RT)$ was approximated by the equation:

$$\log P\left(\frac{E}{RT}\right) = -2.315 - 0.4567\left(\frac{E}{RT}\right) \tag{5}$$

So that:

$$-\log\beta = 0.4567\left(\frac{E}{RT}\right) + \text{constant} \tag{6}$$

Hence, the activation energy is calculated from the thermogravimetric data obtained at different heating rates. The frequency factor is calculated from the equation:

$$\log A = \log g(\alpha)\left[\frac{E}{\beta R} P\left(\frac{E}{RT}\right)\right] \tag{7}$$

Thus, it is obvious that the calculation of E is independent of the reaction model used to describe the reaction, whereas the frequency factor depends on the determined form of $g(\alpha)$.

In the composite method of dynamic data analysis, the results obtained not only at different heating rates but also with different fractional reaction values are superimposed on one master curve [11,12,18–21]. The method employs multiple sets of non-isothermal data and uses all (α, T, β_i) values obtained at the different heating rates, β_i. The use of single-heating rate methods should be very limited and the application of multi-set methods is expected to enrich kinetics with a deeper insight into the multi-step nature of solid-state reactions [22–24].

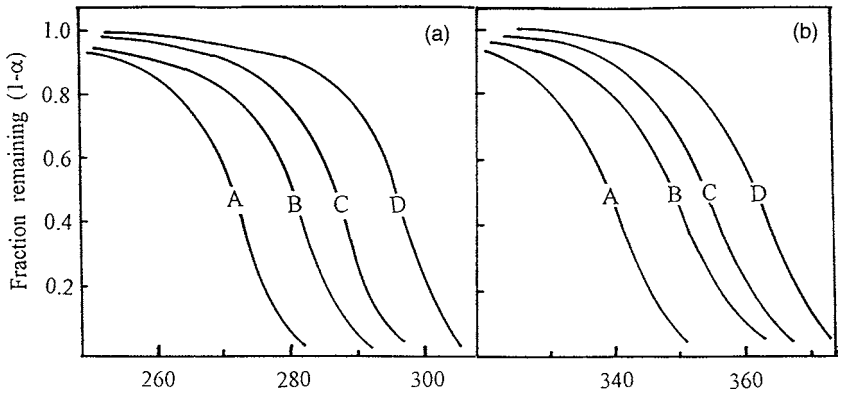

Fig. 4. Dynamic measurements for the thermal decomposition of CuC_2O_4–$ZnC_2O_4{\cdot}2H_2O$ (1:1 mole ratios) mixture in air. Decomposition of: (a) CuC_2O_4 to CuO and (b) ZnC_2O_4 to ZnO. Heating rate: curve A, 1 °C min^{-1}; curve B, 2 °C min^{-1}; curve C, 3 °C min^{-1} and curve D, 5 °C min^{-1}.

The integral form of the equation showing the temperature dependence of the kinetic model function $g(\alpha)$ is rewritten in a form that provides a plot of all non-isothermal data on a single master straight line for the correct reaction model. For example, in the composite method I, the modified Coats–Redfern equation [16] was rewritten in the form:

$$\ln\left[\frac{\beta g(\alpha)}{T^2}\right] = \ln\left(\frac{AR}{E}\right) - \frac{E}{RT} \quad (8)$$

Hence, the dependence of $\ln[\beta g(\alpha)/T^2]$ calculated for different α values at their respective β values, on $1/T$ must give rise to a single master straight line for the correct form of $g(\alpha)$, and a single activation energy and frequency factor can be readily calculated. In a similar way, in the composite method II, Doyle's equation [17] has been rewritten in the form:

$$\log g(\alpha)\beta = \left[\log\frac{AE}{R} - 2.315\right] - 0.4567\frac{E}{RT} \quad (9)$$

Again, the dependence of $\log g(\alpha)\beta$, calculated for the different α values at their respective β values on $1/T$ must give rise to a single master straight line for the correct form of $g(\alpha)$. Vyazovkin and Wight [25] pointed out that the use of the model-free approach is a trustworthy way of obtaining a reliable result from both non-isothermal and isothermal data. Although, the composite method involves a model-fitting kinetic approach, however it does not assume a particular reaction model, but it allow us to choose the model function that gives the best representation of all (α, T, β_i) values obtained at the different heating rate experiments. Deviation from a straight line relationship are interpreted in terms of multi-step reaction mechanism [12,15,26].

Fig. 4 shows representative weight changes as a function of temperature obtained from the dynamic measurements of the oxalate decomposition steps. A computer program [19] was used for the kinetic analysis of non-isothermal data according to the two composite methods using the different models of heterogeneous solid state reactions [12] listed in Table 1. The data can be entered manually or from a data file and the results can be printed out, plotted and saved. The results of calculation allow us to choose the kinetic mechanism which best fits the data and gives the highest correlation coefficient and the lowest standard deviation. The program also calculates the activation energy E and the frequency factor A from the slope and intercept of the linear fit line. The results always show that both the composite methods of analysis gave equivalent curves and nearly identical values for the activation parameters. The values of the activation parameters of the non-isothermal decomposition of CuC_2O_4 and ZnC_2O_4 in their mixture, calculated according to the composite method II, assuming different kinetic models are reported in Table 2. From the table, it is clear that the kinetics of the reaction are best described by the Avrami–Erofeev random nucleation model (A_2), in which the reaction is controlled by initial random nucleation followed by overlapping growth in two dimensions. The

Table 1
Kinetic equations examined in this work

Reaction model	$g(\alpha)$	Symbol
One-dimensional diffusion	α^2	D_1
Two-dimensional diffusion	$\alpha + (1-\alpha)\ln(1-\alpha)$	D_2
Jander equation, three-dimensional diffusion	$[1-(1-\alpha)^{1/3}]^2$	D_3
Ginsling–Braunshtein equation, three-dimensional diffusion	$(1-2/3\alpha)-(1-\alpha)^{2/3}$	D_4
Two-dimensional phase boundary reaction	$[1-(1-\alpha)^{1/2}]$	R_2
Three-dimensional phase boundary reaction	$[1-(1-\alpha)^{1/3}]$	R_3
First order kinetic, Mampel unimolecular law	$[-\ln(1-\alpha)]$	F_1
Random nucleation: Avrami equation	$[-\ln(1-\alpha)]^{1/2}$	A_2
Random nucleation: Erofeev equation	$[-\ln(1-\alpha)]^{1/3}$	A_3
Exponential law	$\ln\alpha$	E_1

fine-grained decomposition products formed in the first oxalate decomposition step catalyze the reaction as it proceeds. This result is in consistent with the formation of hexagonal crystals (as revealed by SEM experiments) and their subsequent growth in *C*-axis direction. The exponential low and other heterogeneous reaction kinetic models gave a less satisfactory fit to the experimental results. Fig. 5 shows typical composite plots of the non-isothermal data based on Doyle's equation according to (A_2) and (E_1) models. From the figure it is obvious that single master straight line for all (α, T, B_i) values was obtained at different heating rate experiments. Fig. 6 shows a plot of the activation energies estimated by the Ozawa method for the oxalate decomposition steps versus α with 0.1α step. The figure shows approximately constant E with α. So, from the above results it is likely that the rate-limiting step is a single reaction step [11].

Analysis of the dynamic data was also carried out using Coats–Redfern and Ozawa methods, assuming A_2 model, and the results were compared with those obtained using the composite method of analysis. Table 3 shows the results of the activation parameters of the non-isothermal study of the oxalate decomposition steps calculated according to the A_2 model using different computational methods. The values of the activation parameters listed in the case of the Coats–Redfern and the Ozawa methods are the average ones for the data calculated at different heating rates (β) and fractional reaction (α) values, respectively. The integral composite analysis showed the less standard deviation in the calculated experimental parameters. In general, there is a good agreement within experimental errors between the activation parameters calculated according to the composite method and those according to Coats–Redfern method however,

Table 2
Activation parameters of the non-isothermal decomposition in air of CuC_2O_4 and ZnC_2O_4 in their mixture, calculated according to the composite method II, assuming different kinetic models

Model	Decomposition of CuC_2O_4 (step II)			Decomposition of ZnC_2O_4 (step III)		
	E (kJ mol^{-1})	log A (min^{-1})	r^*	E (kJ mol^{-1})	log A (min^{-1})	r^*
D_1	348 ± 20	31.4 ± 4.3	0.896	491 ± 27	14.6 ± 5.2	0.892
D_2	369 ± 22	33.2 ± 4.8	0.860	525 ± 29	14.6 ± 5.7	0.889
D_3	397 ± 25	33.2 ± 5.4	0.848	568 ± 33	14.6 ± 6.4	0.884
D_4	379 ± 23	33.4 ± 5.0	0.856	539 ± 31	14.6 ± 5.9	0.888
R_2	208 ± 7	18.2 ± 1.6	0.946	294 ± 9	23.3 ± 1.7	0.965
R_3	215 ± 8	18.7 ± 1.7	0.939	304 ± 9	24.0 ± 1.8	0.962
F_1	229 ± 10	20.7 ± 2.1	0.923	328 ± 11	26.6 ± 2.2	0.953
A_2	131 ± 4	11.4 ± 0.8	0.983	184 ± 3	14.5 ± 0.7	0.986
A_3	98 ± 5	8.2 ± 1.1	0.883	137 ± 7	10.4 ± 1.3	0.913
E_1	118 ± 27	12.0 ± 5.8	0.406	193 ± 36	17.2 ± 7.0	0.507

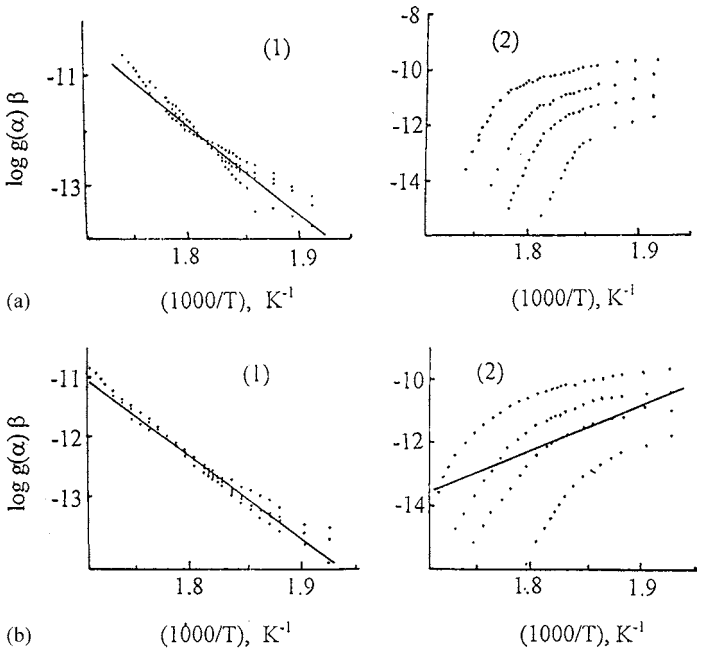

Fig. 5. Composite analysis of TG data for the non-isothermal decomposition in air of (a) CuC_2O_4 and (b) ZnC_2O_4 in their mixture based on Doyle's equation assuming: (1) A_2 model and (2) E_1 model.

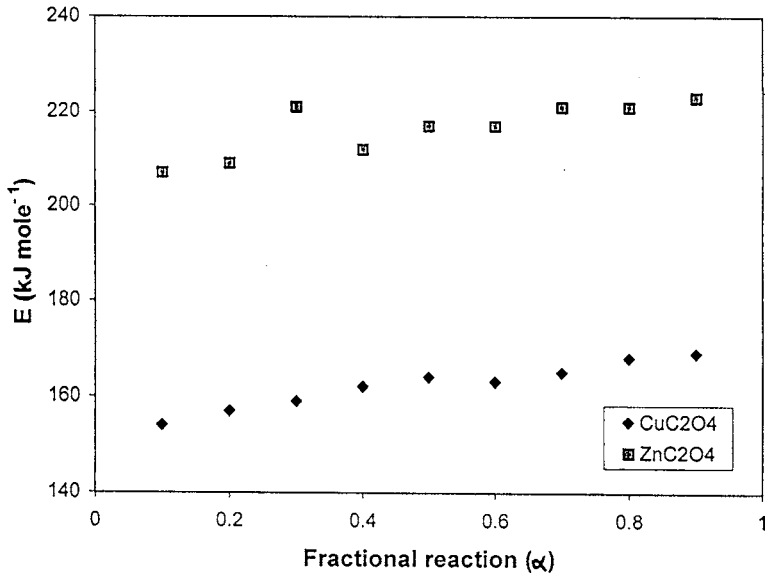

Fig. 6. Plots of the activation energies vs. α calculated by Ozawa method for the thermal decomposition of CuC_2O_4 and ZnC_2O_4 in their mixture.

Table 3
Activation parameters of the non-isothermal decomposition in air of CuC_2O_4 and ZnC_2O_4 in their mixture calculated according to A_2 model

Method of analysis	Decomposition of CuC_2O_4 (step II)		Decomposition of ZnC_2O_4 (step III)	
	E (kJ mol^{-1})	log A (min^{-1})	E (kJ mol^{-1})	log A (min^{-1})
Composite II	131 ± 4	11.4 ± 0.8	184 ± 3	14.5 ± 0.7
Coats–Redfern	126 ± 7	10.9 ± 0.6	178 ± 9	13.9 ± 0.8
Ozawa	162 ± 4	14.0 ± 1.4	216 ± 6	17.2 ± 0.9

the values calculated by the Ozawa method are higher than that calculated by the other two methods which is possibly due to the neglect in the Ozawa method of the reaction mechanism in calculating energies of activation. In many cases, the activation energies estimated by the composite method are, within experimental errors, in good agreement with the values estimated using the model-free method of Ozawa [19–21,27].

Mohamed and Galwey [14] have provided evidence that the decomposition of copper oxalate proceeds via a Cu(I) intermediate with some overlap of stages. The activation energy of the first stage is 140 ± 7 and 180 ± 7 kJ mol^{-1} for the second. Dollimore et al. [28] have been investigated the kinetics and thermal stability of copper oxalate by isothermal and rising temperature experiments in air. The decomposition was found to obey the Avrami–Erofeev (A_2) mechanism with activation energy of 182 ± 10 kJ mol^{-1} in the α range from 0.1 to 0.9. Yankwich and Zavitsanos [10] have reported an activation energy of about 202 ± 13 kJ mol^{-1} for the thermal decomposition of zinc oxalate assuming Avrami–Erofeev equation.

From Table 3 and assuming the composite method II, the activation energy of 184 ± 3 kJ mol^{-1} obtained for the thermal decomposition of zinc oxalate is comparable within experimental errors to that reported by Yankwich and Zavitsanos [10], however, the value of activation energy for the thermal decomposition of copper oxalate is lower than that reported by Dollimore et al. [28]. The decomposition of copper oxalate in nitrogen gives copper metal, and in air the metal powder formed in the decomposition is oxidized to the metal oxide; on the other hand, zinc oxalate gives ZnO on decomposition in both atmospheres [4]. For the oxalates of bivalent metals [5]

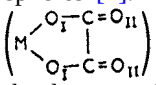

which produces the metal in nitrogen the decomposition temperature represents the temperature at which the M–O_I link is ruptured and will depend critically on the size and charge of metal ion, whereas in those decompositions where the oxide is produced in nitrogen the decomposition temperature represents the energy required to break the C–O_I bond and then will depend less critically on the nature of cation. Also, the extent to which the M–O_I bond is covalent depends on the electronegativity of the metal. The electronegativity of copper (1.9) is more than that of zinc (1.6) [29] and consequently, the addition of zinc ions to CuC_2O_4 will results in an increased positive charge on the copper ion, and a less covalent type of bond thus occurs in the mixed oxalate than in pure CuC_2O_4. This results in weakening of the Cu–O bond and a lowering in activation energy of CuC_2O_4 decomposition.

Acknowledgements

The author would like to thank Prof. Dr. El-H.M. Diefallah for the useful discussion. Thanks are also due to Dr. A.A. El-Bellihi for doing SEM experiments.

References

[1] T.L. Reitz, S. Ahmed, M. Krumpelt, R. Kumar, H.H. Kinn, J. Mol. Catal. A 162 (2000) 275.
[2] J.D. Choi, G.M. Choi, Sens. Actuators B 69 (2000) 120.
[3] N.A.M. Deraz, Colloids Surf. A 190 (2001) 251.
[4] D. Dollimore, D.L. Griffths, J. Therm. Anal. 2 (1970) 229.
[5] D. Dollimore, D.L. Griffths, D. Nicholson, J. Chem. Soc. (1963) 2617.
[6] S. El-Houte, M. El-Sayed Ali, J. Therm. Anal. 37 (1991) 907.
[7] A. Coetzee, D.J. Eve, M.E. Brown, J. Therm. Anal. 39 (1993) 947.
[8] W.W. Wendlandt, Thermal Methods of Analysis, second ed., Wiley/Interscience, New York, 1973.
[9] D. Dollimore, T.A. Evans, Y.F. Lee, Thermochim. Acta 194 (1992) 215.

[10] P.E. Yankwich, P.D. Zavitsanos, J. Phys. Chem. 69 (1965) 918.
[11] El-H.M. Diefallah, M.A. Gabal, A.A. El-Bellihi, N.A. Eissa, Thermochim. Acta 376 (2001) 43.
[12] El-H.M. Diefallah, Thermochim. Acta 202 (1992) 1.
[13] V. Osvaldo, C. Francisco, S. Giullermo, V. Arturo, C. Gerardo, Appl. Surf. Sci. 161 (2000) 27.
[14] M.A. Mohamed, A.K. Galwey, Thermochim. Acta 217 (1993) 263.
[15] T. Ozawa, Bull. Chem. Soc. Jpn. 38 (1965) 1881.
[16] A.W. Coats, J.P. Redfern, Nature 20 (1964) 68.
[17] C.D. Doyle, J. Appl. Polym. Sci. 5 (1961) 285.
[18] S.N. Basahel, A.A. El-Bellihi, El-H.M. Diefallah, J. Therm. Anal. 39 (1993) 87.
[19] El-H.M. Diefallah, A.Y. Obaid, A.H. Qusti, A.A. El-Bellihi, M. Abdel Wahab, M.M. Moustafa, Thermochim. Acta 274 (1996) 165.
[20] A.Y. Obaid, A.O. Alyoubi, A.A. Samarkandy, S.A. Al-Thabaiti, S.A. Al-Juaid, A.A. El-Bellihi, El-H.M. Diefallah, J. Therm. Anal. Cal. 61 (2000) 989.
[21] El-H.M. Diefallah, M.A. Mousa, A.A. El-Bellihi, E.H. El-Mossalamy, G.A. El-Sayed, M.A. Gabal, J. Anal. Appl. Pyrl. 62 (2002) 205.
[22] M. Maciejewski, Thermochim. Acta 355 (2000) 145.
[23] S. Vyazovkin, Thermochim. Acta 355 (2000) 155.
[24] A.K. Burnham, Thermochim. Acta 355 (2000) 165.
[25] S. Vyazovkin, C.A. Wight, Thermochim. Acta 340–341 (1999) 53.
[26] M.E. Brown, M. Maciejewski, S. Vyazovkin, R. Nomen, J. Sempere, A. Burnham, J. Opfermann, R. Strey, H.L. Anderson, A. Kemmler, R. Kenleers, J. Janssens, H.O. Desseyn, C.R. Li, T.B. Tang, B. Roduit, J. Malek, T. Mitsuhashi, Thermochim. Acta 355 (2000) 125.
[27] El-H.M. Diefallah, S.N. Basahel, A.A. El-Bellihi, Thermochim. Acta 290 (1996) 123.
[28] D. Dollimore, T.A. Evans, Y.F. Lee, Thermochim. Acta 194 (1992) 215.
[29] J.A. Dean, Lange's Hand Book of Chemistry, 12th ed., Mc Graw-Hill, New York, 1979.